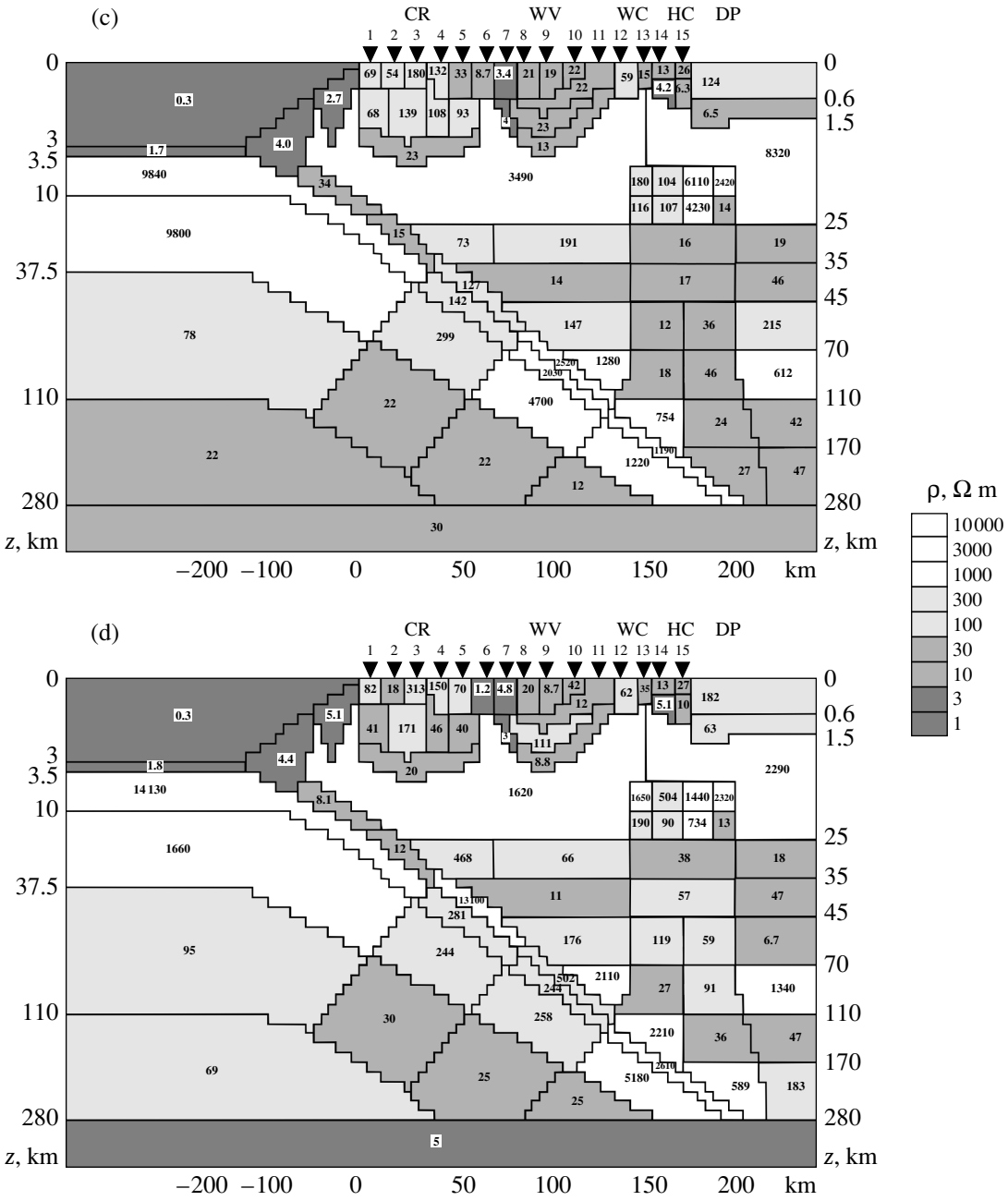

Fig. 20. (Contd.)

agreement of the model with observations. A remarkable feature of the TP model is the conducting continental asthenosphere and the vertical low-resistivity zone that branches from the asthenosphere and crosses the continental crust in the High Cascade region. This feature distinguishes the TP model from EMSLAB-I and EMSLAB-II and makes it similar to the predictive CASCADIA model; in the High Cascades, the latter delineates a vertical high-temperature zone of wet and dry melting that is evidently characterized by low resistivities.

Inversion of $\varphi^{\parallel}$. At this stage, we checked the tipper inversion results. To avoid difficulties related to near-surface distortions of the curves $\rho^{\parallel}$, we restricted ourselves to the inversion of the curves $\varphi^{\parallel}$, which satisfy the dispersion relations. The TP model, obtained from the tipper inversion, was used as a starting model. The inversion of longitudinal phases yielded the TE model, shown in Fig. 20c. The phase misfit (the rms deviation of model phases from observed values) in this model is 5–10 times smaller than the phase amplitude (the difference between the maximum and minimum phase values), indicating good agreement of the model with observations. As distinct from the TP model, the TE continental crust includes a better delineated conducting

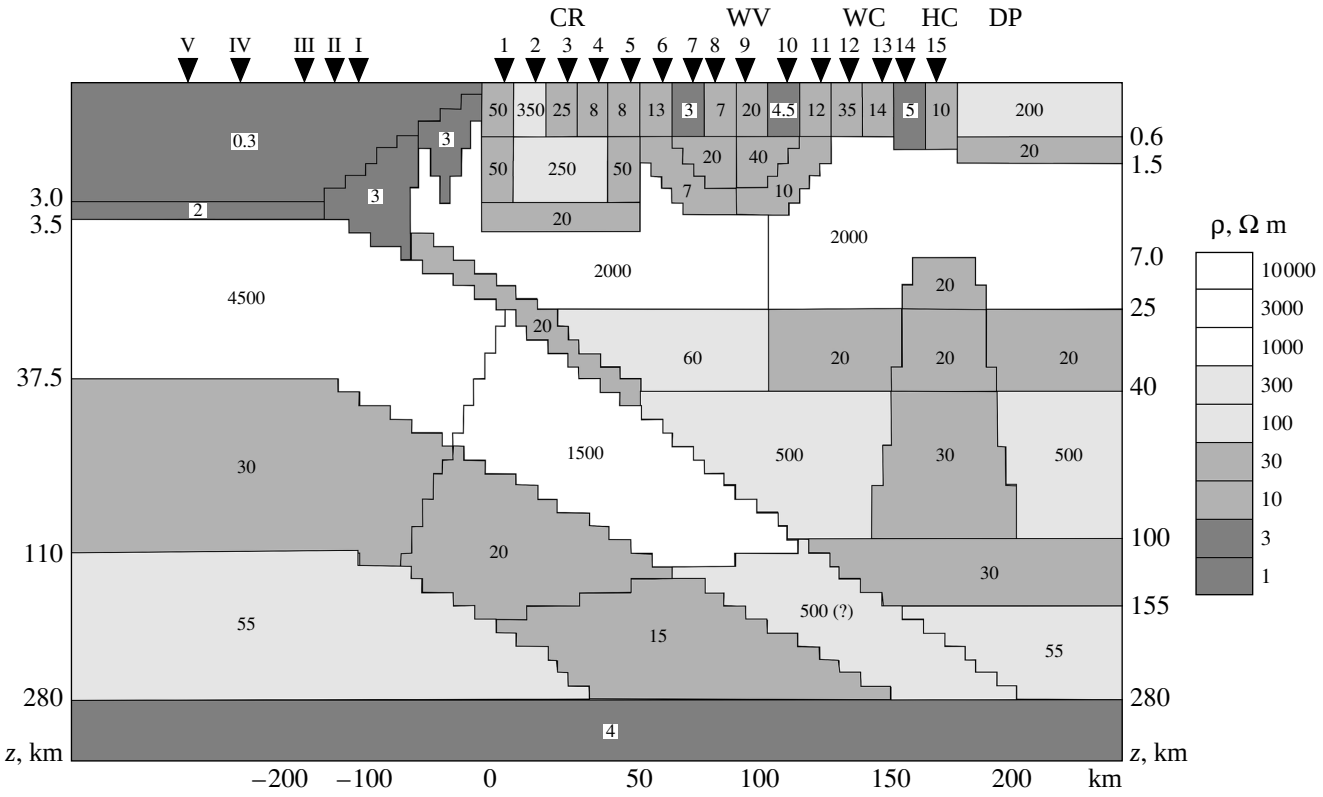

Fig. 21. Final EMSLAB-III model (resistivity values in units of Ω m are shown within blocks): I–V, soundings on the ocean floor; 1–15, soundings on the continent. CR, Coast Range; WV, Willamette Valley; WC, Western Cascades; HC, High Cascades; DP, Deschutes Plateau.

layer (ρ = 14–46 Ω m) in a depth interval of 35–45 km, whereas the subvertical conducting zone (ρ = 12–46 Ω m) in a depth interval of 45–110 km, bounded by layers with resistivities of 147–1260 Ω m to the west and 215–612 Ω m to the east, is localized with a higher contrast. One may state that the TE model is an updated TP model.

Inversion of $\rho^{\perp}$ and $\varphi^{\perp}$. At this stage, we inverted the TM-mode, which is less sensitive to conducting zones in the crust and mantle but is more effective in resolving the structure of the junction zone between the slab and crustal conducting layer and provides more reliable estimates of the resistivity in the upper consolidated crust. In inverting the TM-mode, the TE model, obtained from the inversion of phases $\varphi^{\parallel}$, was taken as a starting model. The inversion of transverse apparent resistivities and phases of the transverse impedance yielded the TM model shown in Fig. 20d. In this model, the misfits of transverse apparent resistivities at most points vary within 6–12%, and the phase misfits are 7–10 times smaller than the phase amplitude (the difference between the maximum and minimum phase values). The TM model inherits the main features of the starting TE model (albeit with some deviations). The following implications of the TM model are noteworthy. First, no well-conducting junction is present between the conducting slab and the crustal conducting layer. Second, the upper consolidated crust of the continent has a resistivity of about 2000 Ω m, indicating that it is fractured.

Note that the TM-mode inversion is essentially dependent on the choice of the starting model. If the START model is taken as the initial one, the TM-mode inversion yields a model in which the continental asthenosphere is absent. This is evidently due to the low sensitivity of the TM-mode to deep conducting structures. In this case, active is the same mechanism that gave rise to the model EMSLAB-I, devoid of the continental asthenosphere, in [Wannamaker *et al.*, 1989b].

Synthesis. At this stage, we analyzed the TP, TE, and TM models and constructed the general EMSLAB-III model, smoothing insignificant details and enlarging blocks on the basis of information characterizing the effect of individual blocks on the MVS and MTS characteristics. All changes were made in an interactive regime, with the calculation of local misfits and with the correction of boundaries and resistivities. The resulting general model shown in Fig. 21 provides a coherent geoelectric image of the subduction zone. The extent of its agreement with observed data is seen from Fig. 22, where the model curves $\rho^{\perp}$, $\rho^{\parallel}$, $\varphi^{\perp}$, $\varphi^{\parallel}$, $\mathrm{Re}\, W_{zy}$,

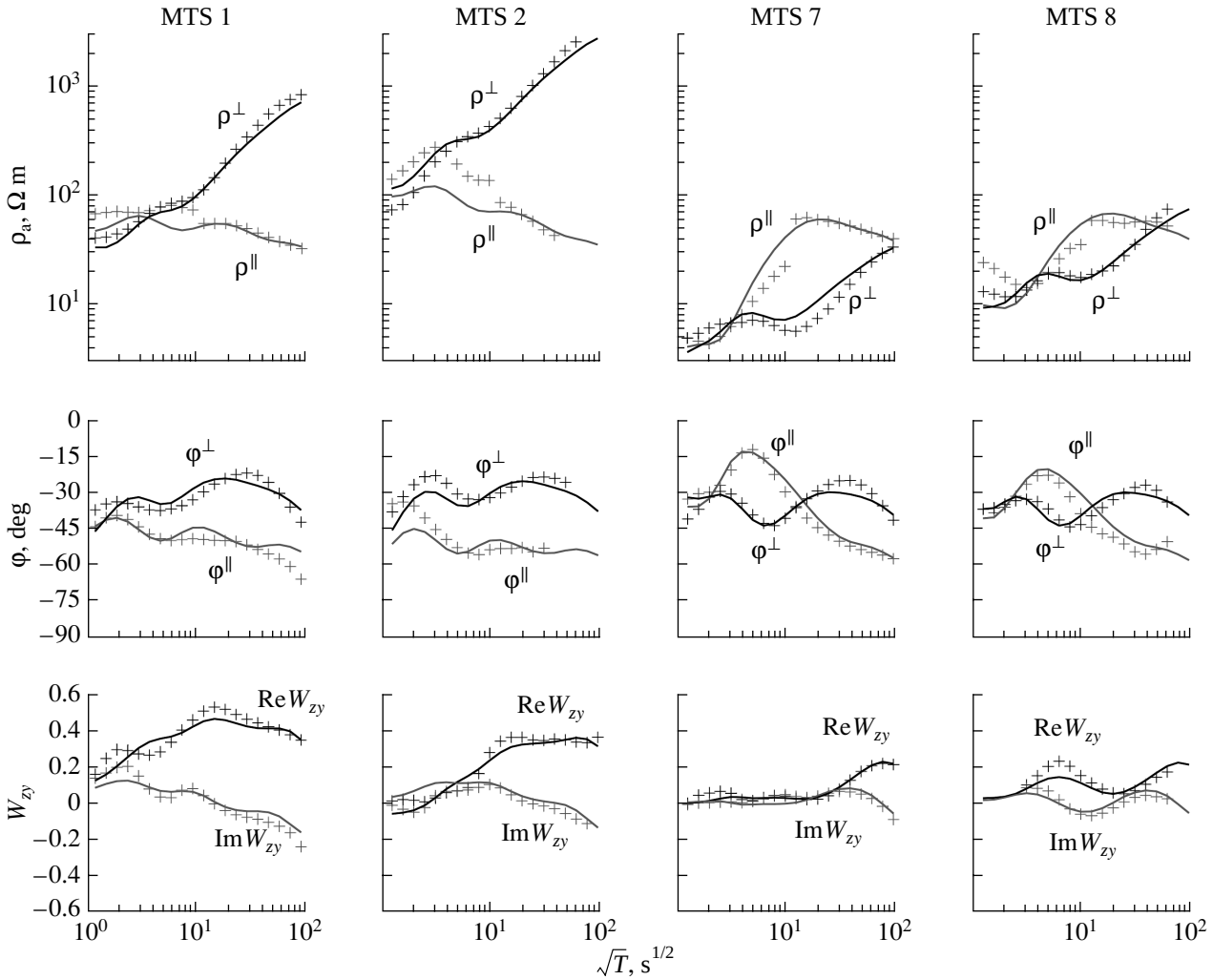

Fig. 22. Comparison of the observed MTS and MVS curves with the curves calculated from the EMSLAB-III model: (*1*) observations; (*2*) EMSLAB-III model.

and $\mathrm{Im}\,W_{zy}$ are compared with the observed curves (the static distortion in the observed curves $\rho^\parallel$ was removed by a vertical shift of their low-frequency branches). The model curves agree well with the observed curves at the majority of points.

In its oceanic part, the EMSLAB-III model is close to EMSLAB-I and EMSLAB-II and exhibits a thick oceanic asthenosphere in a depth interval of 37.5–110 km. The structure of the continental part of EMSLAB-III is distinguished by the following significant elements:

a crustal conducting layer (ρ = 20 Ω m, a depth interval of 25–40 km) and a conducting asthenosphere (30 Ω m, 100–155 km) are distinctly resolved;

the crustal and asthenospheric conductors are connected by a columnlike conducting body (20–30 Ω m) crossing the lithosphere and reaching depths of about 7 km in the volcanic zone of the High Cascades;

the subducting slab, in a depth interval of 4–40 km contains a thin inclined conductor (20 Ω m) separated from the crustal conducting layer by a higher-resistivity zone (60 Ω m); apparently, the crustal conducting layer is unrelated to slab fluids and has a deep origin.

The reliability of these elements is supported by the fact that the elimination of any of them noticeably increases the model misfits.

These features of the continental section make the EMSLAB-III and predictive CASCADIA models similar. The fluid regime of the subduction zone is clearly observable here. The subducting slab entraps fluid-saturated low-resistivity rocks of the ocean floor. As the slab moves down, the released free water migrates through the shear zone (the contact zone between the subducting oceanic and stable continental plates). The dehydration (the release of bound water) developing in the slab at depths of 30–40 km supplies fluids to the mantle and causes the wet melting of asthenospheric material. The low-resistivity melts move upward

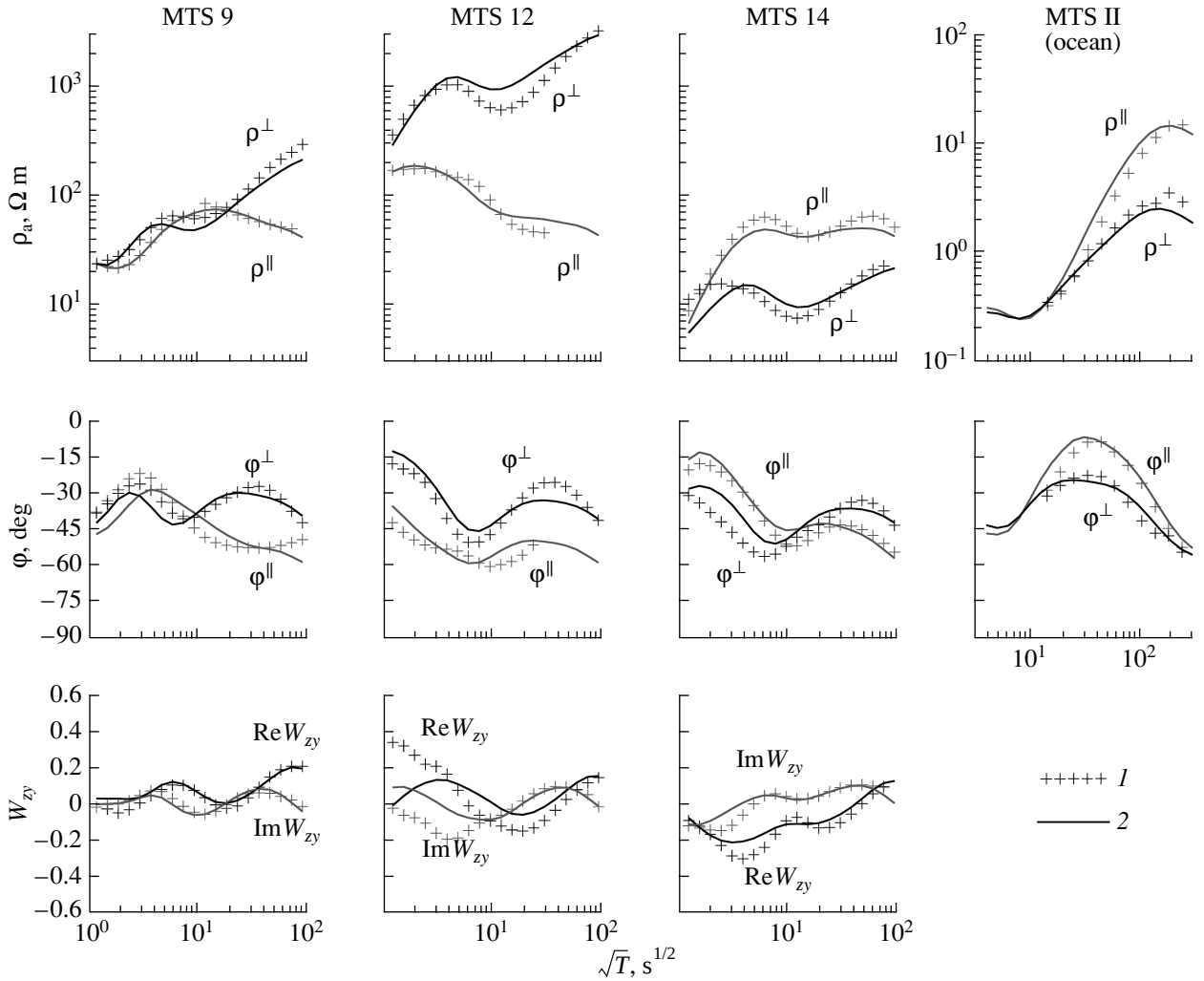

Fig. 22. (Contd.)

through the lithosphere and form a volcanic arc. The heating of the lithosphere activates dehydration in the lower crust, producing the crustal conducting layer.

All this confirms the validity of the predictions underlying the CASCADIA model.

CONCLUSION

Theoretical and experimental results indicate that the MVS method can play a significant role in the development of geoelectric studies. Its main advantage consists in the fact that the magnetic field distortions caused by near-surface inhomogeneities attenuate with decreasing frequency and do not spoil the information on structures of the crust and upper mantle. This makes the results of electromagnetic studies more reliable and better constrained. The development of the MVS method should be regarded as a promising problem of modern geophysics.

Presently, we are at the very beginning of this research, and many questions remain unanswered. What is the best way to organize qualitative analysis of MVS data that accounts most adequately for horizontal and vertical variations in the electrical conductivity? What is the resolution of tippers with respect to these variations? How rapidly do the magnetovariational near-surface effects attenuate at low frequencies? What is the sensitivity of tippers to deep structures in the crust and mantle? Which geoelectric conditions are favorable for the application of the MVS method? What are the conditions at which tippers admit a 2-D approximation of 3-D structures? Such is the list of problems, far from being complete, whose solution is crucial for the progress of MVS.

Answers to many questions can be obtained with the further accumulation of experience in studies in various geological provinces. Here, we should emphasize that a necessary condition for the MVS application is the

presence of conducting inhomogeneities that play the role of deep local sources of electromagnetic field.

The main goal of this paper was to attract the attention of geophysicists to the potentialities of the MVS method and to problems whose solution is indispensable to the practical realization of these potentialities.

ACKNOWLEDGMENTS

We are grateful to P. Weidelt and U. Schmucker for discussions stimulating this work. This work was supported by the Russian Foundation for Basic Research, project nos. 02-05-64079 and 03-05-64167.

REFERENCES

Bahr, K., Interpretation of Magnetotelluric Impedance Tensor: Regional Induction and Local Telluric Distortion, *J. Geophys.*, 1988, vol. 62, pp 119–127.

Berdichevsky, M.N. and Zhdanov, M.S., *Advanced Theory of Deep Geomagnetic Sounding*, Amsterdam: Elsevier, 1984.

Berdichevsky, M.N. and Dmitriev, V.I., *Magnitotelluricheskoe zondirovanie gorizontal'no-odnorodnykh sred* (Magnetotelluric Sounding of Horizontally Homogeneous Media), Moscow: Nedra, 1991.

Berdichevsky, M.N., Koldaev, D.S., and Yakovlev, A.G., Magnetotelluric Sounding on an Ocean Coast, *Fiz. Zemli*, 1992, no. 6, pp. 87–96.

Berdichevsky, M.N., Dmitriev, V.I., and Pozdnjakova, E.E., On Two-Dimensional Interpretation of Magnetotelluric Soundings, *Geophys. J. Int.*, 1998, vol. 133, pp. 585–606.

Berdichevsky, M.N., Vanyan, L.L., and Koshurnikov, A.V., Magnetotelluric Sounding in the Baikal Rift Zone, *Izvestiya, Phys. Solid Earth*, 1999, vol. 35, pp. 793–814.

Berdichevsky, M.N. and Dmitriev, V.I., *Magnetotellurics in the Context of the Theory of Ill-Posed Problems*, Tulsa: SEG, 2002.

Bur'yanov, V.B., Gordienko, V.V., Kulik, S.N., and Logvinov, I.M., *Kompleksnoe geofizicheskoe izuchenie tektonosfery kontinentov* (Multidisciplinary Geophysical Study of the Continental Tectonosphere), Kiev: Naukova Dumka, 1983.

Caldwell, T.G., Bibby, H.M., and Brown, C., The Magnetotelluric Phase Tensor—A Method of Distortion Analysis for 3D Regional Conductivity Structures, *Abstracts of 16th Workshop on EM Induction in the Earth*, Santa Fe, EM12-4.

Connard, G., Couch, R., Keeling, K., *et al.*, Abyssal Plain and Continental Net-Objective Sedimentary Thickness, *Western North American Continental Margin and Adjacent Ocean Floor off Oregon and Washington. Atlas 1 Ocean Margin Drilling Program*, L.D. Kulm *et al.*, Eds., Regional Atlas Series: Marine Science International, Sheet 7, 1984a.

Connard, G., Couch, R., Pitts, G.S., and Troseth, S., Bathymetry and Topography, *Western North American Continental Margin and Adjacent Ocean Floor off Oregon and Washington. Atlas 1 Ocean Margin Drilling Program*, L.D. Kulm *et al.*, Eds., Regional Atlas Series: Marine Science International. Sheet 1, 1984b.

Dmitriev, V.I., *Elektromagnitnye polya v neodnorodnykh sredakh* (Electromagnetic Fields in Inhomogeneous Media), Moscow: MGU, 1969.

Dmitriev, V.I., Inverse Problems in Electrodynamical Prospecting, *Ill-Posed Problems in the Natural Sciences*, Moscow: Mir Publishers, 1987, pp. 77–101.

Dmitriev, V.I. and Mershchikova, N.A., Synthesis of the Magnetotelluric Field, *Fiz. Zemli*, 2002, no. 11, pp. 69–75.

Groom, R.W. and Bailey, R.C., Decomposition of Magnetotelluric Impedance Tensor in the Presence of Local Three-Dimensional Galvanic Distortion, *J. Geophys. Res.*, 1989, vol. 94, no. B2, pp. 1913–1925.

Gusarov, A.L., On the Uniqueness of the Magnetotelluric Data Inversion in a Two-Dimensional Medium, *Matematicheskie modeli v geofizike* (Mathematical Models in Geophysics), Moscow: MGU, 1981, pp. 31–61.

Jones, A.G., Static Shift of Magnetotelluric Data and Its Removal in a Sedimentary Basin Environment, *Geophysics*, 1988, vol. 53, no. 7, pp. 967–978.

Nowozynski, K. and Pushkarev, P.Yu., The Efficiency Analysis of Programs for Two-Dimensional Inversion of Magnetotelluric Data, *Izvestiya, Physics of the Solid Earth*, 2001, vol. 37, pp. 503–516.

Osipova, I.L., Berdichevsky, M.N., Vanyan, L.L., and Borisova, V.P., Geoelectric Models of North America, *Geomagn. Issled.*, 1982, no. 29, pp. 117–130.

Pous, J., Queralt, P., and Marcuello, A., Magnetotelluric Signature of the Western Cantabrian Mountains, *Geophys. Res. Lett.*, 2001, vol. 28, no. 9, pp. 1795–1798.

Rasmussen, J. and Humphries, G., Tomographic Image of the Juan de Fuca Plate beneath Washington and Western Oregon Using Teleseismic *P*-Wave Travel Times, *Geophys. Res. Lett.*, 1988, no. 15, pp. 1417–1420.

Roecker, S.W., Sabitova, T.M., Vinnik, L.P., *et al.*, Three-Dimensional Elastic Wave Velocity Structure of Western and Central Tien Shan, *J. Geophys. Res.*, 1993, vol. 98, no. B9, pp. 15 579–15 795.

Rokityansky, I.I., *Geoelectromagnetic Investigations of the Earth's Crust and Mantle*, Berlin: Springer, 1982.

Romanyuk, T.V., Mooney, W.D., and Blakely, R.J., A Tectonic–Geophysical Model of the Cascadian Subduction Zone in North America, *Geotektonika*, 2001, no. 3, pp. 88–110.

Siripunvaraporn, W. and Egbert, G., An Efficient Data Subspace Inversion Method for 2-D Magnetotelluric Data, *Geophysics*, 2000, vol. 65, pp. 791–803.

Trapeznikov, Yu.A., Andreeva, E.V., Batalev, V.Yu., *et al.*, Magnetotelluric Sounding in the Kyrgyz Tien Shan, *Fiz. Zemli*, 1997, no. 1, pp. 3–20.

Trehu, A.M., Asudeh, I., Brocher, T.M., *et al.*, Crustal Architecture of the Cascadia Forearc, *Science*, 1994, vol. 265, pp. 237–243.

Vanyan, L.L., *Osnovy elektromagnitnykh zondirovanii* (Fundamentals of Electromagnetic Sounding), Moscow: Nedra, 1965.

Vanyan, L.L., Varentsov, I.M., Golubev, N.G., and Sokolova, E.Yu., Construction of Induction Magnetotelluric Curves from Profile Geomagnetic Data for the Study of Electrical Conductivity of the Continental Asthenosphere in the EMSLAB Experiment, *Fiz. Zemli*, 1997, no. 10, pp. 33–46.

Vanyan, L.L., Varentsov, I.M., Golubev, N.G., and Sokolova, E.Yu., Derivation of Simultaneous Geomagnetic Field Components from Tipper Arrays, *Izvestiya, Physics of the Solid Earth*, 1998, vol. 34, pp. 779–786.

Vanyan, L.L., Berdichevsky, M.N., Pushkarev, P.Yu., and Romanyuk, T.V., A Geoelectric Model of the Cascadia Subduction Zone, *Izvestiya, Physics of the Solid Earth*, 2002, vol. 38, pp. 816–845.

Varentsov, I.M., A General Approach to the Magnetotelluric Data Inversion in a Piecewise-Continuous Medium, *Izvestiya, Physics of the Solid Earth*, 2002, vol. 38, pp. 913–934.

Varentsov, I.M., Golubev, N.G., Gordienko, V.V., and Sokolova, E.Yu., Study of the Deep Geoelectric Structure along the Lincoln Line (EMSLAB Experiment), *Fiz. Zemli*, 1996, no. 4, pp. 124–144.

Vozoff, K., The Magnetotelluric Method, *Electromagnetic Methods in Applied Geophysics*, Tulsa: SEG, 1991, vol. 2, pp. 641–711.

Wannamaker, P.E., Stodt, J.A., and Rijo, L., A Stable Finite Element Solution for Two-Dimensional Magnetotelluric Modeling, *Geophys. J. R. Astron. Soc.*, 1987, vol. 88, pp. 277–296.

Wannamaker, P.E., Booker, J.R., Filloux, J.H., *et al.*, Magnetotelluric Observations across the Juan de Fuca Subduction System in the EMSLAB Project, *J. Geophys. Res.*, 1989a, vol. 94, no. B10, pp. 14 111–14 125.

Wannamaker, P.E., Booker, J.R., Jones, A.G., *et al.*, Resistivity Cross Section through the Juan de Fuca Subduction System and Its Tectonic Implications, *J. Geophys. Res.*, 1989b, vol. 94, no. B10, pp. 14 127–14 144.

Weaver, C.S. and Michaelson, C.A., Seismicity and Volcanism in the Pacific Northwest: Evidence for the Segmentation of the Juan de Fuca Plate, *Geophys. Res. Lett.*, 1985, vol. 12, pp. 215–218.

Zinger, B.Sh., Corrections for Distortions of Magnetotelluric Fields: Limits of Validity and Static Approach, *Surv. Geophys.*, 1992, vol. 57, pp. 603–622.